



TITLE:

Conduction-Band Structures of Wurtzite ZnO Solid Solutions by First Principles Calculations

AUTHOR(S):

Wang, Z. J.; Tanaka, I.

CITATION:

Wang, Z. J. ...[et al]. Conduction-Band Structures of Wurtzite ZnO Solid Solutions by First Principles Calculations. MATERIALS TRANSACTIONS 2009, 50(5): 1067-1070

ISSUE DATE:

2009-05

URL:

<http://hdl.handle.net/2433/109952>

RIGHT:

Copyright (c) 2009 The Japan Institute of Metals

Materials Transactions, Vol. 50, No. 5 (2009) pp. 1067 to 1070
Special Issue on Nano-Materials Science for Atomic Scale Modification
©2009 The Japan Institute of Metals

Conduction-Band Structures of Wurtzite ZnO Solid Solutions by First Principles Calculations

Z. J. Wang^{1,2,3} and I. Tanaka^{3,4}

¹National Laboratory of Superhard Materials, Jilin University, Changchun, Jilin, 130012, China

²Physics Department, Jilin University, Changchun, Jilin, 130026, P.R.China

³Department of Materials Science and Engineering, Kyoto University, Kyoto 606-8501, Japan

⁴Nanostructures Research Laboratory, Japan Fine Ceramics Center, Nagoya 456-8587, Japan

Solid solutions of $\text{Zn}_{1-x}\text{Cd}_x\text{O}$ and $\text{Zn}_{1-x}\text{Mg}_x\text{O}$ ($0 \leq x \leq 1$) with wurtzite structures are systematically investigated by first principles calculations with special interests on the dependence of energetics and electronic structures on the alloy structure. Alloying ZnO with CdO shows a linear increase in the lattice parameters when we choose energetically favorable alloy structures. On the other hand, they do not show such a linear trend when alloyed with MgO. Formation energy with reference to the end-member oxides of wurtzite structures is positive for $\text{Zn}_{1-x}\text{Cd}_x\text{O}$ alloys, whereas it is slightly negative for $\text{Zn}_{1-x}\text{Mg}_x\text{O}$ alloy. They are consistent with the experimental fact that highly concentrated solid solutions are easier to be formed in $\text{Zn}_{1-x}\text{Mg}_x\text{O}$ alloys. The band gap shows a monotonous decrease in $\text{Zn}_{1-x}\text{Cd}_x\text{O}$ and increase in $\text{Zn}_{1-x}\text{Mg}_x\text{O}$ with the solute concentration. In $\text{Zn}_{1-x}\text{Cd}_x\text{O}$, Cd has an orbital component as large as that of Zn at the bottom of the conduction band. On the other hand, the contribution of Mg is much smaller in $\text{Zn}_{1-x}\text{Mg}_x\text{O}$. They are consistent with the changes in the band gap with the composition. [doi:10.2320/matertrans.MC200816]

(Received November 10, 2008; Accepted January 19, 2009; Published March 25, 2009)

Keywords: zinc oxide, solid solution, semiconductor, electronic ceramics, dopant, band gap, first principles calculation

1. Introduction

ZnO is one of the most promising semiconductor materials for ultraviolet optoelectronic application due to its wide band gap of 3.4 eV and large exciton binding energy of 60 meV.¹⁻³ Divalent metal oxides such as MgO and CdO are often used to alloy with ZnO as a common strategy for band-gap engineering and optical confinement.⁴⁻⁶ $\text{Zn}_{1-x}\text{Mg}_x\text{O}$ and $\text{Zn}_{1-x}\text{Cd}_x\text{O}$ alloys are well known that the addition of CdO in ZnO decreases the band gap whereas that of MgO increases the band gap. Although both MgO and CdO occur in the cubic rocksalt structure under ordinarily conditions, $\text{Zn}_{1-x}\text{Mg}_x\text{O}$ and $\text{Zn}_{1-x}\text{Cd}_x\text{O}$ alloys are accepted to form the wurtzite structure when x is small.⁴⁻⁷ Under meta-stable thin film growth conditions, the maximum concentration of Mg in wurtzite $\text{Zn}_{1-x}\text{Mg}_x\text{O}$ is typically in the range of $x = 0.4$ to 0.6 .⁸⁻¹⁰ On the other hand it is only about 0.1 .^{5,11} for Cd in wurtzite $\text{Zn}_{1-x}\text{Cd}_x\text{O}$ thin film, except for a few cases reporting success of higher solute concentrations under special process conditions.¹²

There have been a number of theoretical studies on the electronic structures and properties of ZnO, MgO and CdO¹³⁻¹⁸ and their pseudo-binary oxide-alloys.¹⁹⁻²⁴ Very recently Fan and coworkers²⁴ reported systematic first principles calculations of $\text{A}_x\text{Zn}_{1-x}\text{O}$ alloys ($\text{A} = \text{Ca}, \text{Cd}, \text{Mg}$) with rocksalt and wurtzite structures. They examined all different alloy structures within a given supercell in order to know the dependence of the energetics, geometry and band-gap on the alloy structures and compositions. However, they did not explicitly investigate the conduction band structure of these alloys, which should play important roles in optoelectronic applications.

In this work, after confirmation of the dependence on the alloy structure of energetics and electronic structures in solid solutions of $\text{Zn}_{1-x}\text{Cd}_x\text{O}$ and $\text{Zn}_{1-x}\text{Mg}_x\text{O}$ ($0 \leq x \leq 1$) with wurtzite structures, we examine the conduction band structures using first principles calculations.

2. Computational Methods

The calculations were made using the plane-wave basis projector augmented wave (PAW) method²⁵ as implemented in the VASP code.²⁶⁻²⁸ Generalized gradient approximation (GGA) as parameterized by Perdew and Wang (PW91) was used.²⁹ The plane-wave energy cutoff was chosen to be 500 eV. The Brillouin-zone (BZ) integrations in the electron density and the total energy were made using a set of $4 \times 4 \times 4$ k -points of Monkhorst-Pack type³⁰ for 16-atom $\text{Zn}_{1-x}\text{Cd}_x\text{O}$ and $\text{Zn}_{1-x}\text{Mg}_x\text{O}$ supercells. The cell volume and all the ionic positions were relaxed until the residual forces became less than 0.001 eV/nm.

Figure 1 shows the structure of the 16-atom supercell used in the present study, which corresponds to $2 \times 2 \times 1$ of the conventional wurtzite cell. The numbered atoms are Zn, Cd, or Mg, and the dark atoms are O. All different alloy models within the 16-atom supercell are shown in Table 1. All of them were employed for the first principles calculations.

3. Results and Discussion

Lattice parameters for wurtzite ZnO by the present calculation were $a = 0.328$ nm, $c = 0.529$ nm and $u = 0.380$. They are in reasonable agreements with those by experiments,³¹ i.e., $a = 0.324$ nm, $c = 0.519$ nm and $u = 0.382$. Lattice parameters of wurtzite CdO were obtained to be $a = 0.368$ nm, $c = 0.581$ nm and $u = 0.384$. They were $a = 0.331$ nm, $c = 0.51$ nm and $u = 0.387$ for wurtzite MgO.

Figure 2 shows the lattice constants of $\text{Zn}_{1-x}\text{Cd}_x\text{O}$ and $\text{Zn}_{1-x}\text{Mg}_x\text{O}$ alloys for all different alloy structures and compositions. The alloy structures corresponding to the lowest total energies for a given composition are highlighted by solid marks. The solid marks in $\text{Zn}_{1-x}\text{Cd}_x\text{O}$ alloys clearly show that both a and c lattice constants have nearly linear relationship with the Cd concentration. In other words, they follow the Vegard's law, which is in good agreement with the

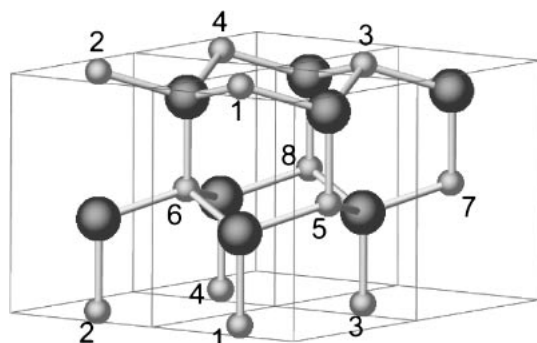


Fig. 1 The 16-atom supercell of a wurtzite structure. Eight cation sites are labeled. The conventional unit cell is shown by thin lines.

Table 1 All different alloy models within the 16-atom supercell. Calculations were made imposing the space group given below.

Composition	Sites occupied by M	Space group	Number of M-M pairs in the cell
Zn_8O_8	null	$P6_3mc$	0
$\text{Zn}_7\text{M}_1\text{O}_8$	8	$P3m1$	0
$\text{Zn}_6\text{M}_2\text{O}_8$	1, 8	$P6_3mc$	1
	1, 5	$Cmc2_1$	1
	1, 2	Pm	1
$\text{Zn}_5\text{M}_3\text{O}_8$	1, 2, 3	$P3m1$	3
	1, 4, 5	Cm	1
	1, 2, 5	Cm	2
$\text{Zn}_4\text{M}_4\text{O}_8$	1, 2, 3, 4	$P3m1$	6
	1, 4, 5, 8	$Pmc2_1$	2
	1, 2, 5, 6	$Pmn2_1$	4
	1, 2, 3, 5	$P3m1$	3
	1, 2, 5, 7	Cc	3
	1, 2, 4, 5	Cm	2
	4, 5, 6, 7, 8	$P3m1$	3
$\text{Zn}_3\text{M}_5\text{O}_8$	2, 3, 6, 7, 8	Cm	4
	3, 4, 6, 7, 8	Cm	5
	2, 3, 4, 5, 6, 7, 8	$P6_3mc$	6
$\text{Zn}_2\text{M}_6\text{O}_8$	2, 3, 4, 6, 7, 8	$Cmc2_1$	7
	3, 4, 5, 6, 7, 8	Pm	6
	1, 2, 3, 4, 5, 7, 8	$P3m1$	9
M_8O_8	8	$P6_3mc$	12
all			

experiment results.¹²⁾ On the other hand in $\text{Zn}_{1-x}\text{Mg}_x\text{O}$, the lattice parameters do not show such linear trends. (Note that the scale of the vertical axis is expanded for $\text{Zn}_{1-x}\text{Mg}_x\text{O}$.) The overall trend of the present results is similar to those in Ref. 24), although some differences can be seen between them. This may be partly ascribed to the use of different exchange-correlation functionals for the calculations and some other computational details. The local density approximation (LDA) is used in Ref. 24), whereas GGA is employed in the present study.

In order to study the stability of $\text{Zn}_{1-x}\text{Cd}_x\text{O}$ and $\text{Zn}_{1-x}\text{Mg}_x\text{O}$ alloys, the formation energies of all alloy configurations were computed. The results are shown in

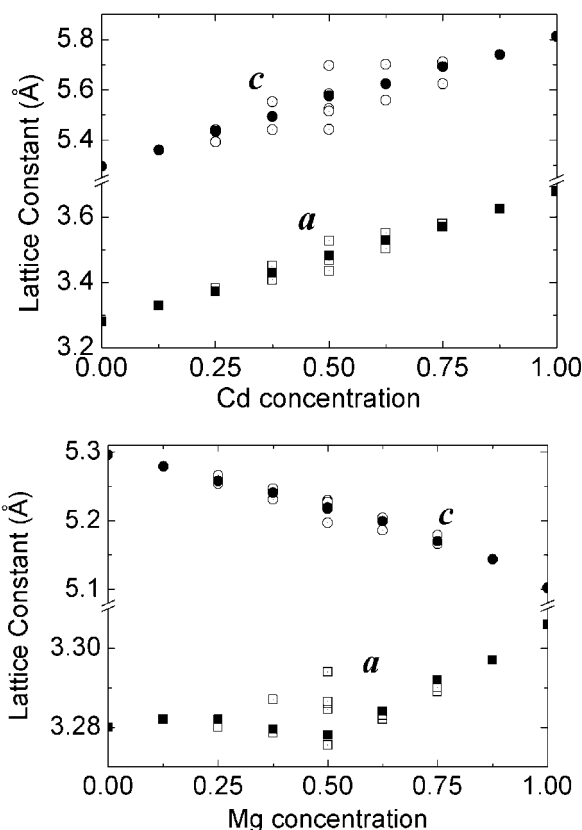


Fig. 2 Theoretical lattice constants of wurtzite ZnO alloys with different solute arrangements. Solid marks correspond to the model showing lowest energy at given solute concentration.

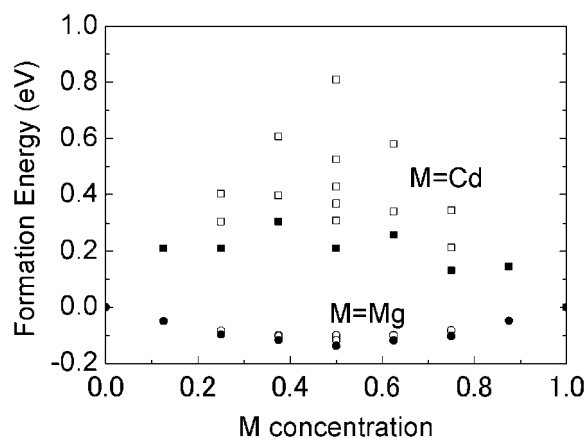


Fig. 3 Theoretical formation energy of wurtzite ZnO alloys with different solute arrangements. Marks denote the same meaning hereafter as Fig. 2.

Fig. 3. Note that three wurtzite crystals, ZnO , MgO and CdO were used as references of the formation energy. Wide scattering of the formation energy with solute configuration is noteworthy for $\text{Zn}_{1-x}\text{Cd}_x\text{O}$. Solid marks correspond to the alloy configuration with the lowest formation energy for a given composition. Formation energy is positive for $\text{Zn}_{1-x}\text{Cd}_x\text{O}$ alloys, whereas it is slightly negative for $\text{Zn}_{1-x}\text{Mg}_x\text{O}$ alloys. They are consistent with the experimental fact that highly concentrated solid solutions are easier to be formed in $\text{Zn}_{1-x}\text{Mg}_x\text{O}$. The present results agree with those in Ref. 24).

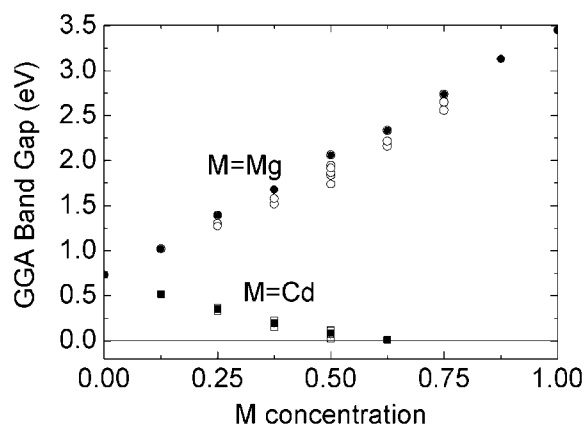


Fig. 4 GGA band-gap of wurtzite ZnO alloys with different solute arrangements. Marks denote the same meaning hereafter as Fig. 2.

The band structures of $\text{Zn}_{1-x}\text{M}_x\text{O}$ ($\text{M} = \text{Cd}, \text{Mg}$) alloys were calculated along lines connecting high-symmetry points in the BZ. Our results shows that both the top of the valence band and the bottom of the conduction band are located at the Γ point ($k = 0$), which indicates the presence of direct band gaps in all of the alloys examined in the present study. The band gaps of the $\text{Zn}_{1-x}\text{Cd}_x\text{O}$ and $\text{Zn}_{1-x}\text{Mg}_x\text{O}$ alloys are shown in Fig. 4. The band gap of undoped ZnO in the present study is 0.73 eV, which is significantly smaller than that by experiments. The band gap vanishes in CdO. Such errors are typical for first principles calculations with the GGA or LDA. For $\text{Zn}_{1-x}\text{Cd}_x\text{O}$ alloys, negative band gaps are omitted from the plot. Although the absolute values of the gap are significantly underestimated, their dependences on solute concentration well agree with experimental data available in literature.^{10,12)}

In order to quantify the electronic structures at the bottom of the conduction band, the fractions of cationic s-orbitals are examined. The fractions of Cd5s and Mg3s increase and that of Zn4s decreases nearly linearly with the increase of the M-concentration as shown in Fig. 5. The bottom of the conduction band gradually changes from Zn4s to Cd5s/Mg3s characters with the M concentration. The increment is larger in Cd doping as compared to the Mg doping. The changes in the conduction band structure can be well visualized by plotting the wave function at the bottom of the conduction band (Γ -point). Figure 6 compares the squared wave functions for ZnO, $\text{Zn}_{7/8}\text{Mg}_{1/8}\text{O}$ and $\text{Zn}_{7/8}\text{Cd}_{1/8}\text{O}$. As for $\text{Zn}_{7/8}\text{M}_{1/8}\text{O}$ ($\text{M} = \text{Cd}, \text{Mg}$), the alloy structure is determined uniquely within the 16-atoms supercell as can be learned from Table 1. The wave functions are plotted on the (0001) plane on which cations number 5 to 8 are periodically located (see Fig. 1). In $\text{Zn}_{7/8}\text{Cd}_{1/8}\text{O}$, Cd shows a contribution as large as that of Zn at the bottom of the conduction band. On the other hand, the contribution of Mg is much smaller in $\text{Zn}_{7/8}\text{Mg}_{1/8}\text{O}$. This is related to the change in the band gap due to the presence of the solute.

4. Conclusion

Solid solutions of wurtzite ZnO with MgO and CdO are systematically investigated by first principles calculations. Results can be summarized as follows:

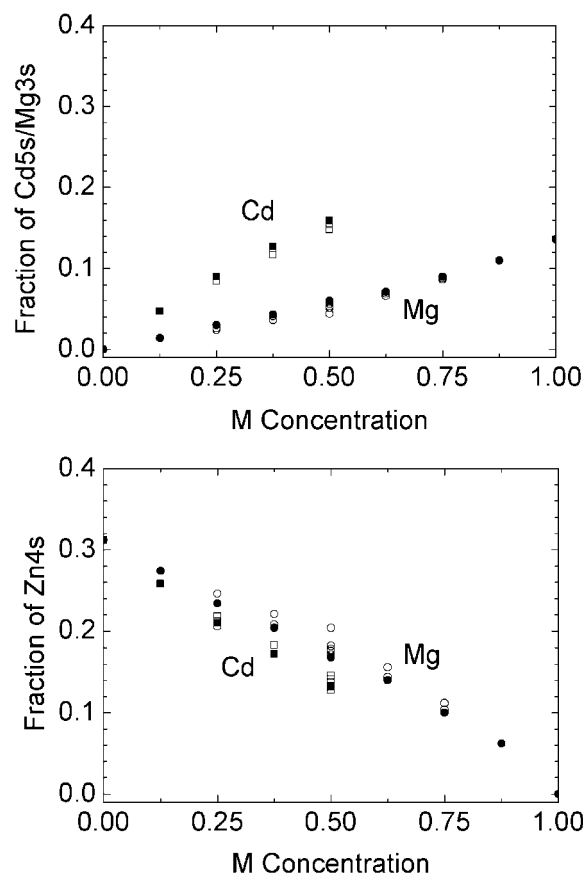


Fig. 5 Orbital population of the state at the bottom of the conduction band at the Γ -Point ($k = 0$).

- (1) The lattice parameters of $\text{Zn}_{1-x}\text{Cd}_x\text{O}$ alloys show a linear increase with the Cd concentration when we choose energetically favorable alloy structures. On the other hand, they do not show such a linear trend in $\text{Zn}_{1-x}\text{Mg}_x\text{O}$ alloys.
- (2) Formation energy with reference to the end-member oxides of wurtzite structures is positive for $\text{Zn}_{1-x}\text{Cd}_x\text{O}$ alloys, whereas it is slightly negative for $\text{Zn}_{1-x}\text{Mg}_x\text{O}$ alloy. They are consistent with the experimental fact that highly concentrated solid solutions are easier to be formed in $\text{Zn}_{1-x}\text{Mg}_x\text{O}$ alloys.
- (3) Band gap shows a monotonous increase in $\text{Zn}_{1-x}\text{Mg}_x\text{O}$ and decrease in $\text{Zn}_{1-x}\text{Cd}_x\text{O}$ with the solute concentration. Although the absolute values of the gap are significantly underestimated, their dependences on the solute concentration well agree with experimental data available in literature.
- (4) In $\text{Zn}_{1-x}\text{Mg}_x\text{O}$, Mg makes a small contribution to the wave function at the bottom of the conduction band. On the other hand, the contribution of Cd is comparable to that of Zn in $\text{Zn}_{1-x}\text{Cd}_x\text{O}$. They are consistent with the changes in the band gap with the composition.

Acknowledgments

The authors would like to thank Fumiyasu Oba for his helpful discussion and Kazuaki Toyoura for technical assistance. This study was supported by Grant-in-Aid for Scientific Research on Priority Areas of Nano Materials Science for Atomic Scale Modification (No. 474) from Ministry of Education, Culture, Sports, Science and Tech-

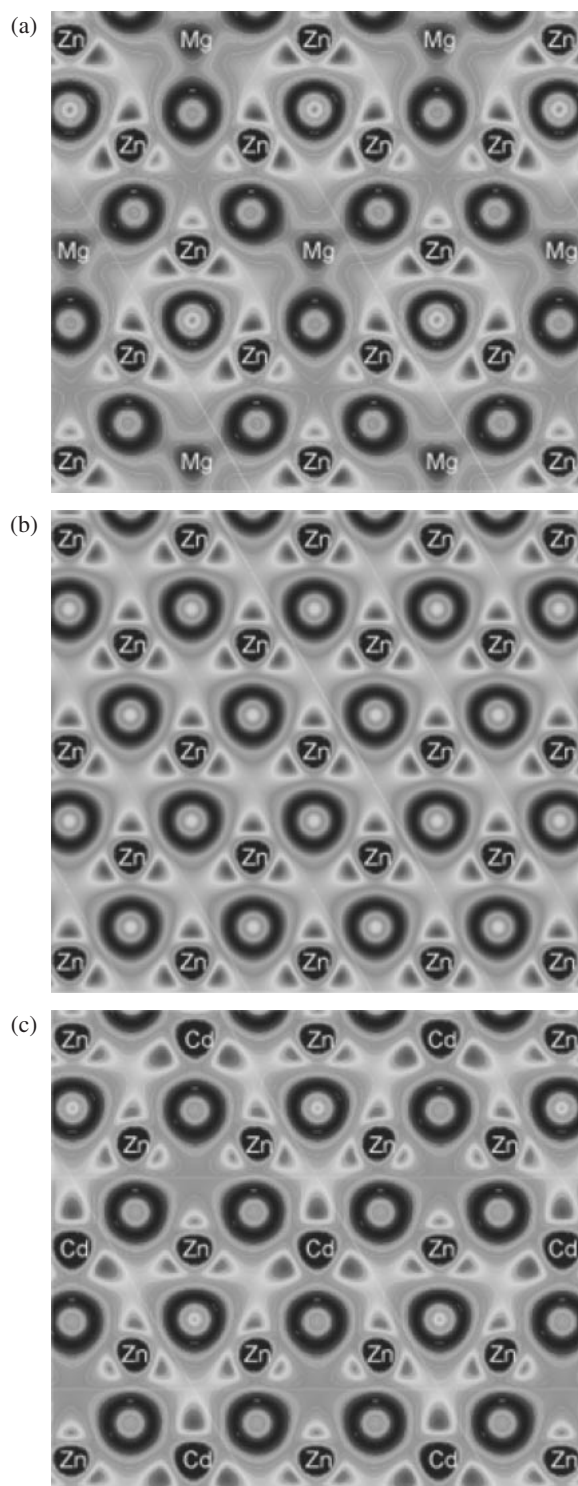


Fig. 6 Squared wave function at the bottom of the conduction band at the Γ -point ($k = 0$) plotted on a (0001) plane. (a) $\text{Zn}_7\text{Mg}_1\text{O}_8$, (b) Zn_8O_8 and (c) $\text{Zn}_7\text{Cd}_1\text{O}_8$.

nology (MEXT) of Japan. Z. J. W was supported by the Scientific Research Foundation for the Returned Overseas Chinese Scholars, State Education Ministry and the Jilin

Province Science and Technology Development Program Project of China (Grant No 20040564).

REFERENCES

- 1) C. Kligshirn: Phys. Status Solidi B **71** (1975) 547.
- 2) Y. S. Park, C. W. Litton, T. C. Collins and D. C. Reynolds: Phys. Rev. **143** (1966) 512.
- 3) D. G. Thomas: J. Phys. Chem. Sol. **15** (1960) 86.
- 4) A. Ohtomo, M. Kawasaki, T. Koida, K. Masubuchi, H. Koinuma, Y. Sakurai, Y. Yoshida, T. Yasuda and Y. Segawa: Appl. Phys. Lett. **72** (1998) 2466.
- 5) T. Makino, Y. Segawa, M. Kawasaki, A. Ohtomo, R. Shiroki, K. Tamura, T. Yasuda and H. Koinuma: Appl. Phys. Lett. **78** (2001) 1237.
- 6) J. J. Chen, F. Ren, Y. Li, D. P. Norton, S. J. Pearton, A. Osinsky, J. W. Dong, P. P. Chow and J. F. Weaver: Appl. Phys. Lett. **87** (2005) 192106.
- 7) H. D. Sun, T. Makino, N. T. Tuan, Y. Segawa, M. Kawasaki, A. Ohtomo, K. Tamura and H. Koinuma: Appl. Phys. Lett. **78** (2001) 2464.
- 8) T. Minemoto, T. Negami, S. Nishiwakib, H. Takakura and Y. Hamakawa: Thin Solid Films **372** (2000) 173.
- 9) W. I. Park, Gyu-Chul Yi and H. M. Jang: Appl. Phys. Lett. **79** (2001) 2022.
- 10) C. X. Cong, B. Yao, G. Z. Xing, Y. P. Xie, L. X. Guan, B. H. Li, X. H. Wang, Z. P. Wei, Z. Z. Zhang, Y. M. Lv, D. Z. Shen and X. W. Fan: Appl. Phys. Lett. **89** (2006) 262108.
- 11) J. Zúñiga-Pérez, V. Muñoz-Sanjose, M. Lorenz, G. Benndorf, S. Heitsch, D. Spemann and M. Grundmann: J. Appl. Phys. **99** (2006) 023514.
- 12) J. Ishihara, A. Nakamura, S. Shigemori, T. Aoki and J. Temmyo: Appl. Phys. Lett. **89** (2006) 091914.
- 13) J. E. Jaffe, J. A. Snyder, Zijing Lin and A. C. Hess: Phys. Rev. B **62** (2000) 1660.
- 14) R. J. Guerrero-Moreno and N. Takeuchi: Phys. Rev. B **66** (2002) 205205.
- 15) A. Schleife, F. Fuchs, J. Furthmüller and F. Bechstedt: Phys. Rev. B **73** (2006) 245212.
- 16) A. Janotti, D. Segev and C. G. Van de Walle: Phys. Rev. B **74** (2006) 045202.
- 17) S. Limpijumngong and W. R. L. Lambrecht: Phys. Rev. B **63** (2001) 104103.
- 18) F. Oba, A. Togo, I. Tanaka, J. Paier and G. Kresse: Phys. Rev. B **77** (2008) 245202.
- 19) A. Malashevich and D. Vanderbilt: Phys. Rev. B **75** (2007) 045106.
- 20) B. Amrani, R. Ahmed and F. El Haj Hassan: Comp. Mater. Sci. **40** (2007) 66.
- 21) H. Rozale, B. Bouhafs and P. Ruterana: Superlattice. Microst. **42** (2007) 165.
- 22) A. Seko, F. Oba, A. Kuwabara and I. Tanaka: Phys. Rev. B **72** (2005) 024107.
- 23) Y. Z. Zhu, G. D. Chen, H. Ye, A. Walsh, C. Y. Moon and S.-H. Wei: Phys. Rev. B **77** (2008) 245209.
- 24) X. F. Fan, H. D. Sun, Z. X. Shen, Jer-LaiKuo and Y. M. Lu: J. Phys. Condens. Matter **20** (2008) 235221.
- 25) P. E. Blöchl: Phys. Rev. B **50** (1994) 17953.
- 26) G. Kresse and J. Hafner: Phys. Rev. B **48** (1993) 13115.
- 27) G. Kresse and J. Furthmüller: Phys. Rev. B **54** (1996) 11169.
- 28) G. Kresse and D. Joubert: Phys. Rev. B **59** (1999) 1758.
- 29) J. P. Perdew: *Electronic Structure of Solids '91*, ed. by P. Ziesche and H. Eschrig (Akademie, Berlin, 1991) p. 11.
- 30) H. J. Monkhorst and J. D. Pack: Phys. Rev. B **13** (1976) 5188.
- 31) J. Albertsson, S. C. Abrahams and A. Kvik: Acta Crystallogr. B **45** (1989) 34.